

The formation of a collisionless shock

ANTOINE BRET,^{1,2} ANNE STOCKEM,³ FREDERICO FIÚZA,³ ERICA PÉREZ ÁLVARO,^{1,2}
CHARLES RUYER,⁴ RAMESH NARAYAN,⁵ AND LUÍS O. SILVA³

¹ETSI Industriales, Universidad de Castilla-La Mancha, Ciudad Real, Spain

²Instituto de Investigaciones Energéticas y Aplicaciones Industriales, Campus Universitario de Ciudad Real, Ciudad Real, Spain

³GoLP/Instituto de Plasmas e Fusão Nuclear – Laboratório Associado, Instituto Superior Técnico, Lisboa, Portugal

⁴CEA, DAM, DIF F-91297 Arpajon, France

⁵Harvard-Smithsonian Center for Astrophysics, Cambridge, Massachusetts

(RECEIVED 20 March 2013; ACCEPTED 20 March 2013)

Abstract

Collisionless shocks are key processes in astrophysics where the energy dissipation at the shock front is provided by collective plasma effects rather than particle collisions. While numerous simulations and laser-plasma experiments have shown they can result from the encounter of two plasma shells, a first principle theory of the shock formation is still lacking. In this respect, a series of 2D Particle-In-Cells simulations have been performed of two identical cold colliding pair plasmas. The simplicity of this system allows for an accurate analytical tracking of the physics. To start with, the Weibel-filamentation instability is triggered in the overlapping region, which generates a turbulent region after a saturation time τ_s . The incoming flow then piles-up in this region, building-up the shock density region according to some nonlinear processes, which will be the subject of future works. By evaluating the seed field giving rise to the instability, we derive an analytical expression for τ_s in good agreement with simulations. In view of the importance of the filamentation instability, we show a static magnetic field can cancel it if and only if it is perfectly aligned with the flow.

Keywords: Collisionless shocks; Weibel instability; Plasma fluctuations

INTRODUCTION

Shocks constitute a fundamental process in many areas of physics ranging from inertial fusion to astrophysics (Betti *et al.*, 2007; Canaud *et al.*, 2012). In a typical fluid shock, upstream particles slow down at the shock front by experiencing an increase of collision frequency. The width of the shock front is therefore equal to a few collisional mean free paths. In a plasma, it has been known since the pioneering work of Sagdeev (1966) that shock-like solutions exist even in the absence of collisions between particles. In this case, the dissipation needed at the shock front to slow down the upstream flow is provided by collective plasma phenomena. The bow shock of the earth magnetosphere within the solar wind provides a perfect natural illustration of such process, as its front thickness has been measured a few tens of km (Bale *et al.*, 2003; Schwartz *et al.*, 2011), while the mean ion free path at the same location is of the order of the Sun-Earth distance, namely $\sim 10^8$ km (Boyd & Sanderson, 2003).

The interest for collisionless shocks is partly due to their capacity to accelerate particles up to very high energies (Drury, 1983; Blandford, & Eichler 1987). In this respect, they could be the factories where ultra high energy cosmic rays up to 10^{21} eV are generated (Letessier-Selvon & Stanev, 2011). While being accelerated near the shock front, particles emit synchrotron radiation, which has been detected in the X-range in supernovae remnant shock fronts (Warren *et al.*, 2005). It is believed that an ultra-relativistic version of the very same process could explain the origin of gamma ray bursts (GRB) (Piran, 2004).

In recent years, this physics has progressively attracted the interest of the Laser-Plasma community, as it is now possible to generate such shocks in the laboratory from the encounter of two collisionless plasmas shells. As evidenced by numerous computer simulations (Liu *et al.*, 2009; Sarri *et al.*, 2011), such encounters drive instabilities when the shells overlap. As a result, the overlapping region turns into a turbulence where the incoming flow piles up. Depending on the nature of the instability triggered, the resulting shock can be mainly electrostatic or electromagnetic. While electrostatic shocks triggered by two-stream like instabilities have already been observed in laboratory (Romagnani

Address correspondence and reprint requests to: Antoine Bret, ETSI Industriales, Universidad de Castilla-La Mancha, 13071 Ciudad Real, Spain. E-mail: antoineclaude.bret@uclm.es

et al., 2008; Liu et al., 2011), electromagnetic shocks triggered by fast growing electromagnetic instabilities in the relativistic regime are yet to be realized, although favorable conditions for their obtention have been recently obtained in Rochester (Ross et al., 2012). In this later experiment, two opposite CH₂ foils were irradiated with a laser intensity of 10¹⁶ W/cm². As a result, counter-streaming plasmas with peak velocities 2000 km/s = 6 × 10⁻³ c were created. With an interaction length ~8 mm and a mean free path ~27 mm, conditions were met for a shock to form although the interaction time was not long enough.

As previously said, observations of the earth bow shock, laboratory laser-plasma experiments, and numerical simulations are now instrumental in investigating such shocks. On the theory side, the large body of available literature has so far mainly overlooked the formation process, rather focusing on the dynamic of the already formed shock. The present paper aims at filling this gap by providing a detailed theory of collisionless shock formation out of the encounter of two plasma shells. Two-dimensional (2D) particle-in-cells (PIC) simulations have thus been performed of two symmetric, cold, colliding pair plasmas. Note that besides being relevant for GRB's physics, pair plasma avoid having to deal with the proton/electron mass ratio. The simplicity of this system allows for an accurate analytical description of the unstable spectrum involved in the overlapping region. Noteworthy, pair plasma-like experiments are already possible using mixtures of positively and negatively charged C₆₀ (Oohara & Hatakeyama, 2003).

Assessing both the field at saturation and the initial seed field triggering the instability, it has been possible to derive an expression for the instability saturation time in good agreement with the simulations. As will be checked, this saturation time is not the shock formation time, but only a lower bound to the later. Future works will focus on the non-linear processes that pick-up the system at saturation time and build the shock.

PIC SIMULATIONS AND INSTABILITY ANALYSIS

PIC simulations have been used to model the shock formation using the code OSIRIS (Fonseca et al., 2002). A pair plasma with Lorentz factor $\gamma_0 \in [25, 10^4]$ and reduced temperature

$\mu = mc^2/k_B T = 10^6 \gamma_0$ is sent toward a wall where it bounces back and interact with itself (see Fig. 1). This scheme is widely used when modeling the interaction of two identical plasmas and avoids the simulation of the other half of the system (Silva et al., 2003). The particles are injected from the right by a cathode along the x axis with a temporal resolution $\Delta t = 0.025 \sqrt{\gamma_0}/\omega_p$, and reflected at the wall. The 2D box with $L_x = 125 \sqrt{\gamma_0} c/\omega_p$ and $L_y = 5 \sqrt{\gamma_0} c/\omega_p$ has absorbing boundaries for the particles along x and is periodic along y . For the fields, conducting boundaries are used at the perfectly reflecting wall and open boundary conditions at the cathode.

Figure 2 shows the temporal growth of the magnetic energy integrated over the overlapping region, where the right-ward bouncing part interacts with the left-ward plasma. As expected, an initial exponential growth is observed, resulting from the excitation of streaming instabilities. Previous analysis of the unstable spectrum involved (Bret et al., 2005; 2008) have shown that in the present case, the fastest growing modes are found with $k_x = 0$. These are the so-called filamentation, or Weibel, modes, with growth rate (Bret, 2009; Bret et al., 2010),

$$\frac{\delta}{\omega_p} = \frac{v_0}{c} \sqrt{\frac{2}{\gamma_0}} \sim \sqrt{\frac{2}{\gamma_0}}, \quad (1)$$

where ω_p is the plasma frequency of one isolated shell. As evidenced in Figure 2 by the dashed line, the field grows precisely at the expected rate.

In view of the role of the filamentation instability in the present context, an evaluation of the conditions required to cancel it is important. To this day, two factors are known that can suppress this instability in the collisionless regime: thermal spread and magnetic field. For the former, several works have evidenced that temperature can potentially stabilize filamentation beyond a threshold which depends on the distribution functions involved (Silva et al., 2002; Bret & Deutsch, 2006). Regarding the later, early works by Godfrey et al. (1975) showed a static flow-aligned field could stabilize filamentation. Yet, astrophysical settings frequently imply non flow-aligned fields (Sironi & Spitkovsky, 2009). The present cold counter-streaming symmetric system has thus been analyzed accounting for an oblique magnetic field \mathbf{B}_0 . The dispersion equation for the filamentation instability

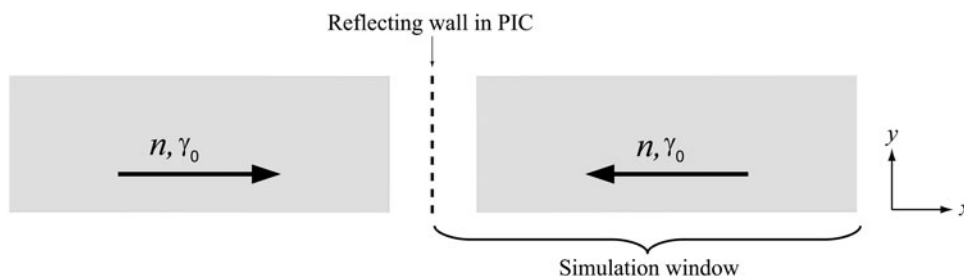


Fig. 1. Two identical pair plasmas collide. Only the right part is simulated. Setting a bouncing wall on the dashed line, the full system can be modeled saving half the computation time.

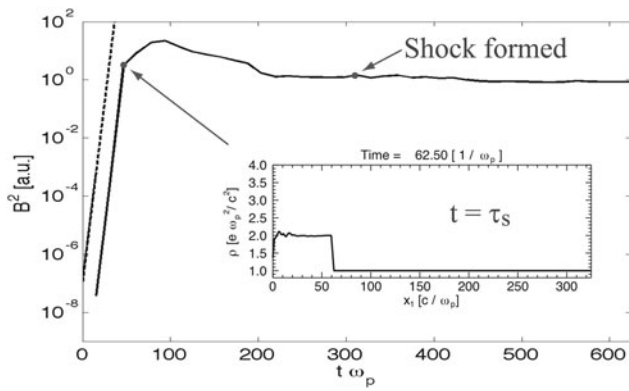


Fig. 2. Growth of the integrated magnetic energy B^2 (arbitrary units) in the overlapping region. The shock forms only *after* the instability saturates at $t = \tau_s$. The insert shows the y -integrated density at $t = \tau_s$. Density is normalized to the one of a single shell.

exhibits a behavior similar to the flow-aligned case: the growth rate in the limit $k_{\perp} = \infty$ tends to a constant, because no kinetic pressure exists to prevent small filaments from pinching. By deriving the dispersion equation in this limit, one finds filamentation growth rate tends to a finite but non zero value, when $B_0 \rightarrow \infty$ with (Bret & Alvaro, 2011),

$$\frac{\delta}{\omega_p} \sim \frac{v_0}{c} \sqrt{\frac{2}{\gamma_0 \sqrt{1 + \gamma_0^2 \cot^2 \theta}}} \quad \text{for } B_0 \gg 2 \frac{v_0 \sqrt{\gamma_0}}{c \cos \theta}, \quad (2)$$

where θ is the angle between the flow and \mathbf{B}_0 . This result emphasizes the robustness of the filamentation instability in realistic scenarios where θ would hardly be exactly zero.

As long as the linear hypothesis is fulfilled, the exponential growth continues. Saturation comes at $t \equiv \tau_s$, when the density perturbation generated is no longer small. As a consequence, the density in the overlapping region at $t \equiv \tau_s$ may be slightly larger than twice the upstream density, but *only* slightly, since perturbations *must* be small at lesser times. Because the Rankine-Hugoniot jump conditions give here a density jump ~ 3.3 , the saturation time is necessarily smaller than the shock formation time. Starting from the saturation time where the “downstream” density is only $2 + \epsilon$, nonlinear processes need to intervene in order to raise it to ~ 3.3 . Leaving this second phase for further studies, we now focus on the determination of τ_s , starting with the assessment of the initial and final field amplitudes.

INITIAL AND FINAL FIELD AMPLITUDES

Assuming the magnetic field grows from an initial amplitude B_i to a final one B_f , the saturation time τ_s is straightforwardly given by,

$$B_f = B_i e^{\delta \tau_s} \quad \Rightarrow \quad \tau_s = \frac{1}{\delta} \ln \left(\frac{B_f}{B_i} \right). \quad (3)$$

The amplitude of the field at saturation has been largely discussed in literature (Davidson *et al.*, 1972; Medvedev & Loeb, 1999). By stating that the linear approximation ceases to be valid when the cyclotron frequency of the particles in the growing field becomes comparable to the growth rate, one can derive

$$\frac{B_f^2}{8\pi} \sim \gamma_0 n m c^2, \quad (4)$$

where n is the density of one isolated shell and m the electron/positron mass.

From the physical point of view, the initial field B_i results from the spontaneous fluctuations continuously emitted and absorbed in the shells. Like a pencil in equilibrium over its tip, it takes a slight deviation from equilibrium to destabilize the system. As they approach each other, each shell presents density fluctuations with $k_x = 0$ associated with the corresponding magnetic fluctuations. As soon as they overlap, these fluctuations result in uncompensated opposite parallel currents instantaneously destabilizing the system (Fried, 1959). The relevant magnetic fluctuation amplitude for B_i is thus the one of a single shell drifting at relativistic velocity. Such calculation has been performed by Yoon (2007) in the non-relativistic regime and recently extended to the relativistic regime by Ruyer and Gremillet (2012). The fluctuations giving rise to the filamentation instability have both k_x and $\omega = 0$. In the regime $1 \ll \gamma_0 \ll \mu$, the $d\omega d^3k$ -energy density they contain is given by,

$$\begin{aligned} \frac{B_{k_{\perp,\omega}}^2(\omega = 0)}{8\pi} &\equiv \frac{B_{k_{\perp,0}}^2}{8\pi} \\ &= \frac{1}{\sqrt{32}\pi} \frac{\gamma_0^3 mc^2}{\sqrt{\mu} \omega_p}, \quad \mu = \frac{mc^2}{k_B T}. \end{aligned} \quad (5)$$

Interestingly, the density $B_{k_{\perp,\omega}}$ is extremely peaked near $\omega = 0$, with a peak width given by,

$$\delta\omega = \frac{\omega_p}{\gamma_0 \sqrt{6\mu}}. \quad (6)$$

In other words, almost all of the energy contained in fluctuations with $k_x = 0$ is concentrated around $\omega = 0$.

In order to reach an evaluation of B_i , Eq. (5) has to be integrated over $d\omega d^3k$. Regarding the ω -integration domain, we just multiply Eq. (5) by the peak width Eq. (6).

Turning now to the \mathbf{k} -integration domain, Eq. (5) has been integrated in the parallel direction between \pm the largest unstable $k_{\parallel,max} = \sqrt{\gamma_0/2}(\omega_p/c)$ (Bret *et al.*, 2010). With respect to the perpendicular direction, it has been found numerically that the fastest growing mode has $k_{\perp} \equiv k_{\perp,m} \sim (\omega_p/c)/\sqrt{\gamma_0}$. We thus simply integrated the energy density in this direction over $[k_{\perp,min}, k_{\perp,max}] = [k_{\perp,m}/2, 3k_{\perp,m}/2]$. Note that such loose approximations are eventually without much consequences as the end result for the saturation time eventually involves their

logarithm. Note also that one fastest wave vector is selected for growth, in spite of the fact that the unstable spectrum for the present cold system does *not* exhibit any local growth-rate extremum at this location (Bret *et al.*, 2010). Further work will be required in order to understand this point.

To summarize, the initial field amplitude B_i reads,

$$\frac{B_i^2}{8\pi} = \int_{k_{\perp, \min}}^{k_{\perp, \max}} 2\pi k_{\perp} dk_{\perp} \int_{-k_{\parallel, \max}}^{k_{\parallel, \max}} dk_{\parallel} \int_{-\delta\omega}^{\delta\omega} d\omega \frac{B_{k_{\perp, 0}}^2}{8\pi}, \quad (7)$$

and a little algebra gives

$$\frac{B_i^2}{8\pi} = \frac{15\sqrt{\pi/6}\sqrt{\gamma_0}}{4} \frac{(\omega_p}{\mu})^3 mc^2. \quad (8)$$

SATURATION TIME

The time to reach saturation follows from Eqs. (3), (4), and (8) and reads,

$$\tau_s \omega_p = \frac{\sqrt{\gamma_0}}{2\sqrt{2}} \ln \left[\frac{4}{15} \sqrt{\frac{6}{\pi}} n \left(\frac{c}{\omega_p} \right)^3 \sqrt{\gamma_0} \mu \right]. \quad (9)$$

Figure 3 displays the comparison of the saturation time τ_s as measured from simulations, with the analytical result above. The agreement found is rather good, given the looseness of the calculations and the difficulty to model the fluctuations level in the simulations. Within the range of expected Lorentz factors in GRB context, namely $\gamma_0 < 10^3$ (Piran, 2004; Nakar *et al.*, 2011), the agreement is very good.

CONCLUSION

We have presented a first principle theory of the formation of a collisionless shock. We focused on the first phase of this process, namely the growth of the dominant instability triggered in the overlapping region, and the time it takes to reach saturation. The analytical expression obtained is in

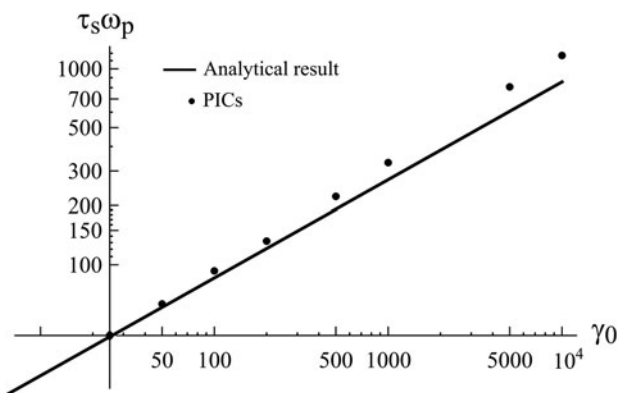


Fig. 3. Comparison of the saturation time τ_s as measured from simulations with the analytical result (9).

good agreement with the simulation and represent therefore a lower bound to the shock formation time. Given the importance of filamentation instability as the shock formation trigger, it has been found that a static magnetic field can cancel it only if it is perfectly aligned with the flow.

Further works will be now dedicated to the exploration of the second phase during which the shock density jump builds up. Hopefully, an understanding of the shock formation will tell if a shock *always* form, and what time and space it takes to do so. These information will help design future shock experiments and constrain the parameters involved in GRB and cosmic ray physics.

ACKNOWLEDGMENTS

This work was supported by projects ENE2009-09276 of the Spanish Ministerio de Educación y Ciencia, the European Research Council (ERC-2010-AdG Grant 267841) and FCT (Portugal) grants PTDC/FIS/111720/2009 and SFRH/BD/38952/2007. Thanks are due to Lorenzo Sironi for useful discussions.

REFERENCES

- BALE, S. D., MOZER, F. S. & HORBURY, T. S. (2003). Density-transition scale at quasiperpendicular collisionless shocks. *Phys. Rev. Lett.* **91**, 265004.
- BETTI, R., ZHOU, C. D., ANDERSON, K. S., PERKINS, L. J., THEOBALD, W. & SOLODOV, A. A. (2007). Shock ignition of thermonuclear fuel with high areal density. *Phys. Rev. Lett.* **98**, 155001.
- BLANDFORD, R. & EICHLER, D. (1987). Particle acceleration at astrophysical shocks: A theory of cosmic ray origin. *Phys. Rep.* **154**, 1.
- BOYD, T. & SANDERSON, J. (2003). *The Physics of Plasmas*. New York, NY: Cambridge University Press.
- BRET, A. (2009). Weibel, two-stream, filamentation, oblique, bell, bune-man... which one grows faster? *Astrophys. J.* **699**, 990.
- BRET, A. & ALVARO, E. P. (2011). Robustness of the filamentation instability as shock mediator in arbitrarily oriented magnetic field. *Phys. Plasma* **18**, 080706.
- BRET, A. & DEUTSCH, C. (2006). Stabilization of the filamentation instability and the anisotropy of the background plasma. *Phys. Plasmas* **13**, 022110.
- BRET, A., FIRPO, M. & DEUTSCH, C. (2005). Bridging the gap between two stream and filamentation instabilities. *Laser Part. Beams* **23**, 375.
- BRET, A., GREMILLET, L., BÉNISTI, D. & LEFEBVRE, E. (2008). Exact relativistic kinetic theory of an electron-beam plasma system: Hierarchy of the competing modes in the system-parameter space. *Phys. Rev. Lett.* **100**, 205008.
- BRET, A., GREMILLET, L. & DIECKMANN, M. E. (2010). Multidimensional electron beam-plasma instabilities in the relativistic regime. *Phys. Plasmas* **17**, 120501.
- CANAUD, B., LAFFITE, S., BRANDON, V. & TEMPORAL, M. (2012). 2d analysis of direct-drive shock-ignited hiper-like target implosions with the full laser megajoule. *Laser Part. Beams* **30**, 183.
- DAVIDSON, R. C., HAMMER, D. A., HABER, I. & WAGNER, C. E. (1972). Nonlinear development of electromagnetic instabilities in anisotropic plasma. *Phys. Fluids* **15**, 317.

- DRURY, L. O. C. (1983). An introduction to the theory of diffusive shock acceleration of energetic particles in tenuous plasmas. *Rpt. Prog. Phys.* **46**, 973.
- FONSECA, R., SILVA, L., TSUNG, F., DECYK, V., LU, W., REN, C., MORI, W., DENG, S., LEE, S., KATSOULEAS, T. & ADAM, J. (2002). Osiris: A three-dimensional, fully relativistic particle in cell code for modeling plasma based accelerators. *Lecture Notes in Comput. Sci.* **2331**, 342.
- FRIED, B. D. (1959). Mechanism for instability of transverse plasma waves. *Phys. Fluids* **2**, 337.
- GODFREY, B. B., SHANAHAN, W. R. & THODE, L. E. (1975). Linear theory of a cold relativistic beam propagating along an external magnetic field. *Phys. Fluids* **18**, 346.
- LETESSIER-SELVON, A. & STANEV, T. (2011). Ultrahigh energy cosmic rays. *Rev. Mod. Phys.* **83**, 907.
- LIU, M.-P., XIE, B.-S., HUANG, Y.-S., LIU, J. & YU, M. (2009). Enhanced ion acceleration by collisionless electrostatic shock in thin foils irradiated by ultraintense laser pulse. *Laser Part. Beams* **27**, 327.
- LIU, X., LI, Y. T., ZHANG, Y., ZHONG, J. Y., ZHENG, W. D., DONG, Q. L., CHEN, M., ZHAO, G., SAKAWA, Y., MORITA, T., KURAMITSU, Y., KATO, T. N., CHEN, L. M., LU, X., MA, J. L., WANG, W. M., SHENG, Z. M., TAKABE, H., RHEE, Y.-J., DING, Y. K., JIANG, S. E., LIU, S. Y., ZHU, J. Q. & ZHANG, J. (2011). Collisionless shockwaves formed by counter-streaming laser-produced plasmas. *N. J. Phys.* **13**, 093001.
- MEDVEDEV, M. V. & LOEB, A. (1999). Generation of magnetic fields in the relativistic shock of gamma-ray burst sources. *Astrophys. J.* **526**, 697.
- NAKAR, E., BRET, A. & MILOSAVLJEVIĆ, M. (2011). Two-stream-like instability in dilute hot relativistic beams and astrophysical relativistic shocks. *Astrophys. J.* **738**, 93.
- OOHARA, W. & HATAKEYAMA, R. (2003). Pair-ion plasma generation using fullerenes. *Phys. Rev. Lett.* **91**, 205005.
- PIRAN, T. (2004). The physics of gamma-ray bursts. *Rev. Mod. Phys.* **76**, 1143.
- ROMAGNANI, L., BULANOV, S., BORGHESI, M., AUDEBERT, P., GAUTHIER, J., LWENBRCK, K., MACKINNON, A., PATEL, P., PRETZLER, G., TONCIAN, T. & et al. (2008). Observation of collisionless shocks in laser-plasma experiments. *Phys. Rev. Lett.* **101**, 025004.
- ROSS, J. S., GLENZER, S. H., AMENDT, P., BERGNER, R., DIVOL, L., KUGLAND, N. L., LANDEN, O. L., PLECHATY, C., REMINGTON, B., RYUTOV, D., ROZMUS, W., FROULA, D. H., FIKSEL, G., SORCE, C., KURAMITSU, Y., MORITA, T., SAKAWA, Y., TAKABE, H., DRAKE, R. P., GROSSKOPF, M., KURANZ, C., GREGORI, G., MEINNECKE, J., MURPHY, C. D., KOENIG, M., PELKA, A., RAVASIO, A., VINCI, T., LIANG, E., PRESURA, R., SPITKOVSKY, A., MINIATI, F. & PARK, H.-S. (2012). Characterizing counter-streaming interpenetrating plasma relevant to astrophysical collisionless shocks. *Phys. Plasmas* **19**, 056501.
- RUYER, C. & GREMILLET, L. (2012). *In Preparation*.
- SAGDEEV, R. Z. (1966). Cooperative phenomena and shock waves in collisionless plasmas. *Rev. Plasma Phys.* **4**, 23.
- SARRI, G., DIECKMANN, M., KOURAKIS, I. & BORGHESI, M. (2011). Generation of a purely electrostatic collisionless shock during the expansion of a dense plasma through a rarefied medium. *Phys. Rev. Lett.* **107**, 025003.
- SCHWARTZ, S. J., HENLEY, E., MITCHELL, J. & KRASNOSELSKIKH, V. (2011). Electron temperature gradient scale at collisionless shocks. *Phys. Rev. Lett.* **107**, 215002.
- SILVA, L. O., FONSECA, R. A., TONGE, J. W., DAWSON, J. M., MORI, W. B., & MEDVEDEV, M. V. (2003). Interpenetrating plasma shells: Nearequipartition magnetic field generation and nonthermal particle acceleration. *Astrophys. J.* **596**, L121–L124.
- SILVA, L. O., FONSECA, R. A., TONGE, J. W., MORI, W. B. & DAWSON, J. M. (2002). On the role of the purely transverse weibel instability in fast ignitor scenarios. *Phys. Plasmas* **9**, 2458.
- SIRONI, L. & SPITKOVSKY, A. (2009). Particle acceleration in relativistic magnetized collisionless pair shocks: Dependence of shock acceleration on magnetic obliquity. *Astrophys. J.* **698**, 1523.
- WARREN, J. S., HUGHES, J. P., BADENES, C., GHAVAMIAN, P., MCKEE, C. F., MOFFETT, D., PLUCINSKY, P. P., RAKOWSKI, C., REYNOSO, E. & SLANE, P. (2005). Cosmic-ray acceleration at the forward shock in Tycho's supernova remnant: Evidence from chandra X-ray observations. *Astrophys. J.* **634**, 376.
- YOON, P. H. (2007). Spontaneous thermal magnetic field fluctuation. *Phys. Plasmas* **14**, 064504.